Supporting information of super-elastic graphene/carbon nanotube aerogels and their application as strain-gauge sensor

Peng Lv, Kehan Yu, Xiaowen Tan, Ruilin Zheng, Yiwen Ni, Zhongyue Wang, Chunxiao Liu, Wei Wei*

School of Optoelectronic Engineering, Nanjing University of Posts & Telecommunications, Nanjing 210023, P.R.China

Graphene/CNT aerogels with various densities were prepared by controlling the GO/fCNT concentration to study the effect of the density on the conductivity and the sensitivity of aerogels. As shown in Fig. S1, the micro-structure of the aerogels became denser and their average pore size tuned to smaller with the increase of GO/fCNT concentration.

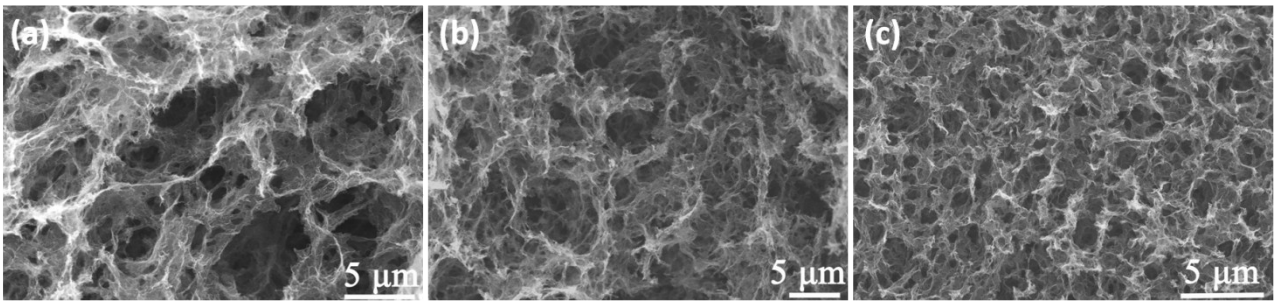


Fig. S1 SEM images of graphene/CNT-4, -6, and -12 aerogels corresponding to GO/fCNT concentration of 4, 6 and 12 mg $mL^{-1}$, respectively.

A graphene aerogel without CNTs were also prepared using similar method with GO concentration of 9 mg $mL^{-1}$, and its density was 15.1 mg $cm^{-3}$. As shown in Fig. S2, the graphene aerogel exhibited a 3D porous structure with the cell dimension in range of 1~5 μm. The zoom-in SEM images indicated that the cellar walls consisted of partially overlapping graphene sheets (Fig. S2b) and wrapping graphene sheets (Fig. S2c). However, the π-π interactions between the adjacent graphene sheets were too weak to construct a macro-scopically 3D graphene with good mechanical strength. The graphene sheets easily moved past each other when the 3D graphene aerogel was under external force.

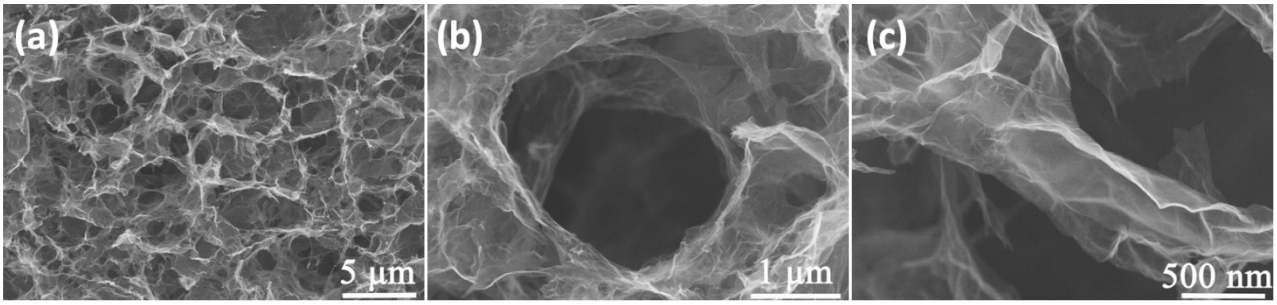


Fig. S2 SEM images of the graphene aerogel without CNTs

Micro-Raman spectroscopy (RM3000, Renishaw) was performed using a laser excitation wavelength of 514.5 nm. XRD were measured by a high resolution X-ray diffraction system (PW1825, Philips) using Cu Kα1 radiation at 40 kV. As shown in Fig. S3a, The pattern of GO displayed a strong (001) diffraction peak at 2θ value of 10.1˚, corresponding to 0.87 nm of interlayer spacing. After hydrothermal process, the XRD pattern of graphene aerogel showed a dominant broad peak at 24.1˚ corresponding to the graphite-like structure (002) instead of the diffraction peak at 10.1˚, indicating that GO had been reduced during the hydrothermal process. And the graphene/CNT aerogel showed the diffraction peak at 24.2˚ similar to graphene aerogel, also suggested that some π-π stacking between graphene sheets and CNTs. The structural change after hydrothermal process was further reflected in the Raman spectra (Fig. S3b). The spectra of GO, graphene aerogel and graphene/CNT aerogel displayed the existence of D and G bands located at 1350-1356 and 1593-1604 $cm^{-1}$, respectively. The intensity ratio of D and G bands ($I_D/I_G$) was 0.881 in GO and 0.921 in GO/fCNT, then increased to 0.992 and 1.043 in graphene aerogel and graphene/CNT aerogel, respectively. The increase in the D band intensity may be attributed to the decrease in the average size of the $sp^2$ domain upon reduction of GO. It was anticipate that the hydrothermal reduction process removed partial oxygen containing functional groups would provide strong π-π interaction between graphene sheets and CNTs, and promoted their aggregation to form the hydrogel.

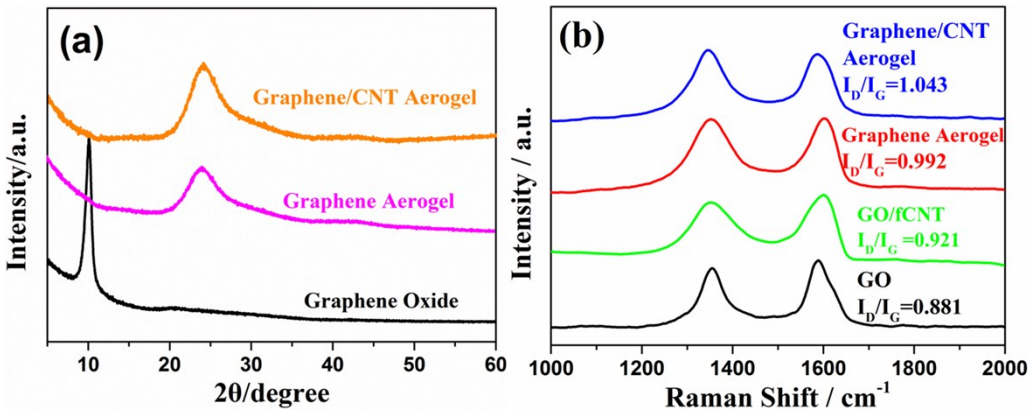


Fig. S3 (a) XRD pattern of graphene/CNT aerogel, graphene aerogel and GO; (b) Raman spectra of graphene/CNT aerogel, graphene aerogel, GO/fCNT and GO

The graphene aerogel could be squeezed into pellet under certain pressure. Once the external pressure was removed, the graphene aerogel deformed permanently indicating a structural collapse (Fig. S4).

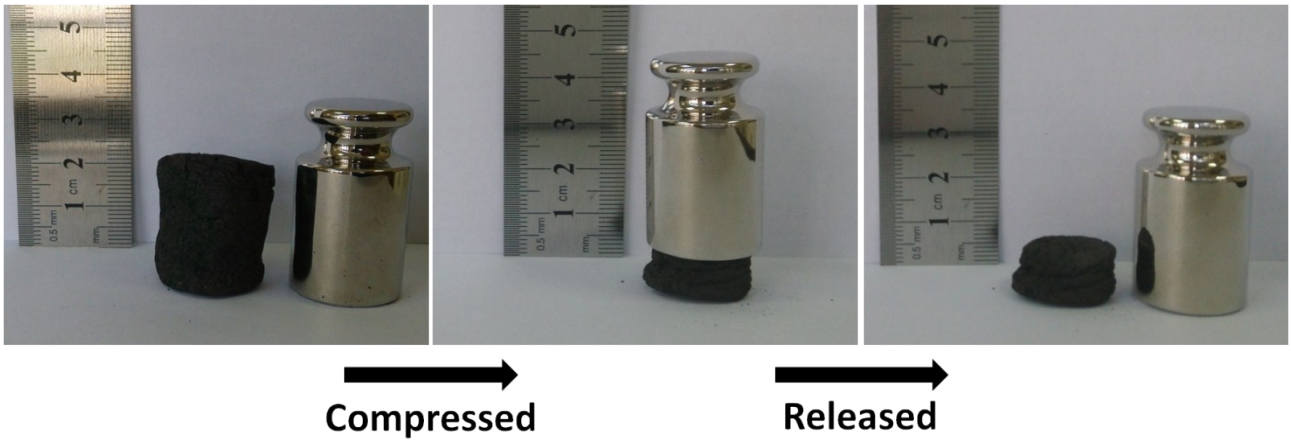


Fig. S4 Digital photographs showing that the graphene aerogel collapsed and could not recover its original shape after compression.

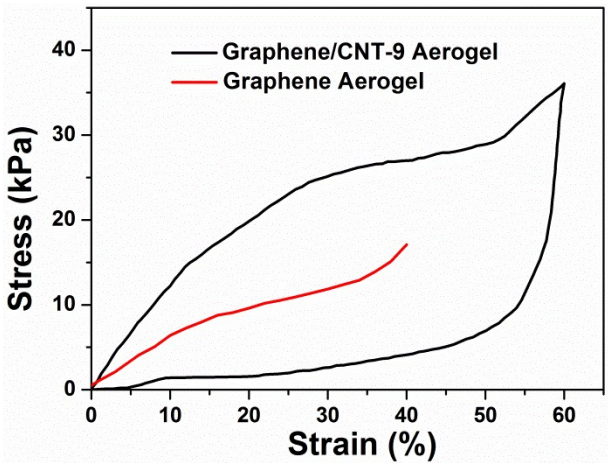


Fig. S5 Stress-strain curves of graphene aerogel without CNTs and graphene/CNT-9 aerogel. The measurement could not carry out during unloading of the graphene aerogel because the permanently deformed during loading to strain of ~40%.

The increased compressive stress of 3D graphene after introducing CNTs into it suggests CNTs can greatly enhance the strength and elastic stiffness of cell walls. The enhancement of aerogels by CNTs is one of the important reasons for the super-elasticity of graphene/CNT aerogels.

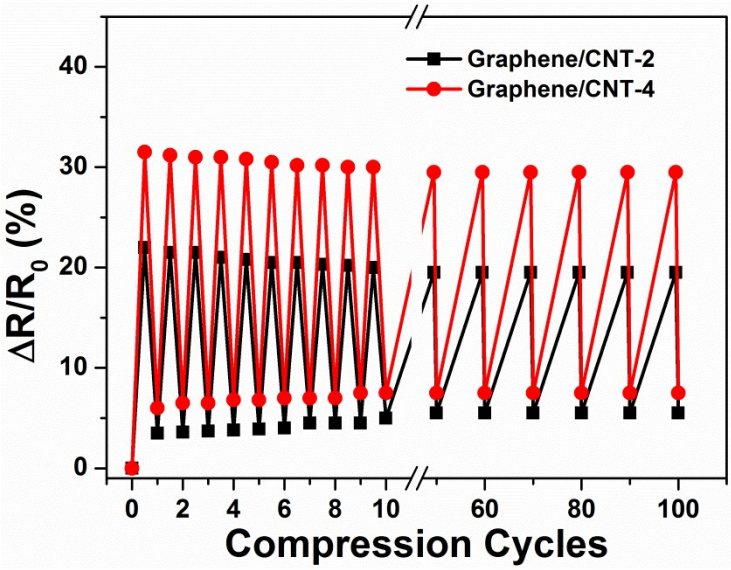


Fig.S6 Electrical resistance change of graphene/CNT-2 and -4 aerogels when repeatedly compressed up to 60% strain for over 100 cycles.